Scale-up considerations of the UBFB solar receiver

Cite as: AIP Conference Proceedings **2126**, 030067 (2019); https://doi.org/10.1063/1.5117579
Published Online: 26 July 2019

Huili Zhang, Shuo Li, Weibin Kong, Gilles Flamant, and Jan Baeyens

Scale-up Considerations of the UBFB Solar Receiver

Huili Zhang[1, a)], Shuo Li[1, b)], Weibin Kong[1, c)] Gilles Flamant[2, d)], Jan Baeyens[3, 4, e)]

[1] *Beijing University of Chemical Technology (BUCT), School of Life Science and Technology,15# Beisanhuan east road, Beijing, China*
[2] *PROMES-CNRS, Route du Four Solaire 7, Odeillo-Font Romeu, France*
[3] *European Powder and Process Technology, Park Tremeland 9, Tremelo, Belgium*
[4] *BUCT, Beijing Advanced Centre of Soft Matter and Engineering, Beijing, China*

[a)]zhhl@mail.buct.edu.cn
[b)]ssurel@163.com
[c)]kongweibin2012@gmail.com
[d)]gilles.flamant@promes.cnrs.fr
[e)]Corresponding author: EuroPPT@gmail.com

Abstract. Concentrated Solar Power plants (CSP) are a promising technology for electricity generation. Indirect particle receivers can operate at high receiver temperatures and foster the application of advanced power generation cycles. The present work specifically considers the scale-up of the CNRS concept, referred to as Upflow Bubbling Fluidized Bed (UBFB) system. Previous papers have provided detailed information concerning the on-sun testing of a single tube and of a 150 kW pilot module consisting of 16 parallel tubes. SiC, a Geldart A type powder, was used and fluidized at superficial gas velocities of ~0.03 to 0.25 m s^{-1}. To scale-up these vertical UBFBs, some phenomena require additional attention. These phenomena are 5-fold, and related to (i) the pressure balance over the receiver and the achievable solids' flux and air velocity relationship; (ii) the efficiency of the vertical transport; (iii) the possible particle choking; (iv) the gas-solid hydrodynamics gradually transforming from a freely bubbling into a slugging mode in long UBFB tubes; and (v) attrition and erosion. These phenomena will be further discussed.

CONCEPT AND TESTING OF THE UBFB RECEIVER

Further to the single tube (36 mm I.D., 0.5 m long) experiments at the solar furnace of PROMES-CNRS in Font Romeu (FR) [1–3], a multi-tube set-up (16 parallel tubes of 29.7mm I.D., each 1 m long) of was investigated [4,5]. Layouts and operation details are presented in the respective publications. The particle feed temperature of the receiver tubes was between 25 and 460 °C. The total exchanger area of the tubes is determined by the set-up geometry. Overall energy balances were established and are illustrated in Fig. 1 together with the results of the single tube experiments. Clearly, the average heat flux of the single and multi-tube set-ups is comparable, confirming the scale-up validity of the single-tube experiments.

SolarPACES 2018
AIP Conf. Proc. 2126, 030067-1–030067-8; https://doi.org/10.1063/1.5117579
Published by AIP Publishing. 978-0-7354-1866-0/$30.00

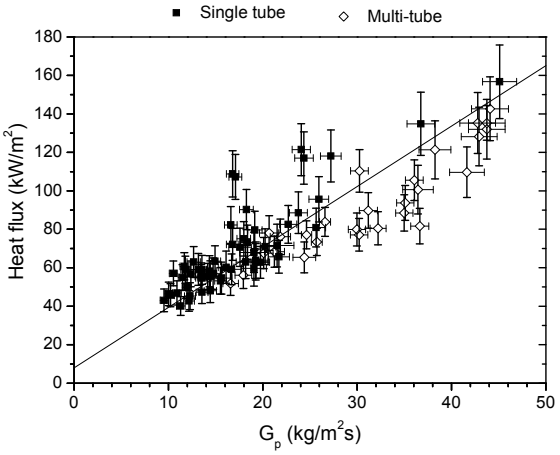

FIGURE 1: Heat flux vs. mass flux in single and multi-tube experiments (Credit: PROMES-CNRS)

INITIAL IMPROVEMENTS

To overcome the high cost of SiC, 58 μm cristobalite of density 2340 kg/m^3 was additionally and subsequently tested in a vertical high temperature electrical furnace using tubes of 46 and 50.09 mm O.D., each 0.5 m long. Operating parameters (temperatures of wall, inlet/outlet particles, and solid flux) were continuously monitored. The absorbed heat was calculated from the heat balance of the particle suspension flow. The tube geometries, including fins in the 50.09 mm O.D., were known, thus enabling the calculation of the heat transfer coefficient. Since using only 4 temperature measurements of the outside wall along the height of the tube, and temperature measurements of the inlet and outlet solids flow, results are less accurate than when using multiple thermocouples as in the PROMES-CNRS on-sun set-ups, but allow a fair determination of an average overall heat transfer coefficient. Bare tubes tested were respectively 46 mm O.D. (wall thickness 2 mm) and 50.09 mm O.D. The 50.09 mm O.D. tube was also manufactured with internal fins, as illustrated in Fig. 2 for wall temperatures up to 685 °C. For comparison and to gather data at higher flux densities at the wall on-sun, single tube experiments (bare and finned tubes) are currently conducted by CNRS using Group A cristobalite and olivine.

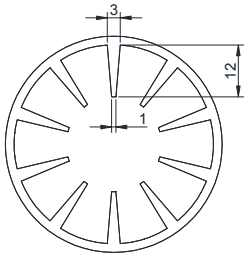

FIGURE 2: Top view of the 50.09 mm O.D. finned tube (dimensions in mm)

Results were previously detailed in Zhang et al. [6], but repeated in Fig. 3.

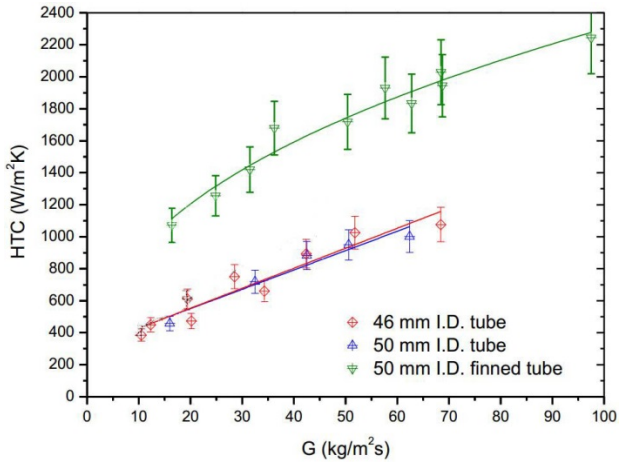

FIGURE 3: Experimental heat transfer coefficient versus solids circulation flux G for different tube geometries [6]

At higher wall temperatures, radiation heat transfer should be added and will increase the experimental values by about 50 (low G) to 150 W/m^{2}K (high G), to achieve a maximum of ~1050 W/m^{2}K for the bare tubes, and ~2200 W/m^{2}K for the finned tube. Heat transfer coefficients for the bare tubes are slightly lower than those obtained by CNRS in 29 and 26 mm. I.D. tubes [1–5]. The decrease of the heat transfer coefficient is however largely compensated by the increase in heat exchanger surface area per meter of tube length, being + 27.7 % for the 46 mm and + 38.9 % for the 50 mm tube. The exposed surface area of the finned tube was 2.835 times the surface area of the bare tube. Experiments moreover give evidence of the fact that solid circulation fluxes up to ~100 kg/m^{2}s are achievable and provide stable operating conditions of the UBFB.

ADDITIONAL SCALING-UP CONSIDERATIONS

Pressure Balance, Achievable Solid Flux and Air Velocity Relationship

The layout of a continuous UBFB loop, as used in e.g. solar receivers, is represented in Fig. 4. The dispenser bed is operated at a fluidization velocity close to the minimum bubbling (U_{mb}) superficial velocity of the powder (~1.2 to 1.5 U_{mb}). The major part of the conveying gas is injected at the bottom of the tube (about 10 cm above its inlet). In the loop, different factors should be considered. The solid fraction, α_p, in the upward part of the circuit (the riser) is lower than α_p in the downcomer parts, being 0.35-0.40 and 0.45-0.50 respectively. Rotary valves RV1 and RV2 not only create an additional pressure drop, but control the bed level of ⑥ and the rate of solid circulation, respectively. The pressurization of hopper ⑥, indicated as ΔP_6, and subsequent downer parts of the circuit add to the pressure balance.

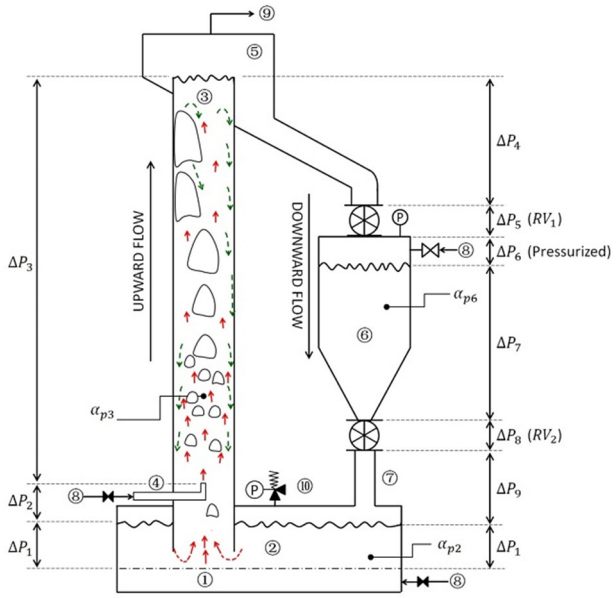

FIGURE 4: Particle movement and pressure balance in the UBFB [7], with bubble and G_s-driven particle upflow; gross particle downflow near the wall; ①windbox; ② fluidized bed dispenser with ⑩ pressure relief valve; ③ up-flow bubbling fluidized bed; ④ secondary air injector; ⑤disengagement chamber; ⑥ pressurized hopper; ⑦downcomer; ⑧ compressed air; ⑨ to fines filtration. RV: rotary valve

To operate the loop in a stable flow mode, driving downflow pressures (including the pressurization of hopper ⑥) should exceed pressure drops of the upflow branch including acceleration and friction losses, ΔP_f. This is represented as follows:

$$\sum_4^9 \Delta P_i + \Delta P_l \geq \sum_2^3 \Delta P_i + \Delta P_f \tag{1}$$

The dispenser bed exerts a pressure on the fluidized solids proportional to the bulk density and the bed height above the inlet of the vertical tube. If this effective bed depth is H_{DB}, the pressure drop exerted is

$$\Delta P_{DB} = \rho_s (1 - \varepsilon) H_{DB} g \tag{2}$$

Since the feeding loop is moreover pressurized at an external pressure ΔP_{ext}, the total driving force is

$$\Delta P = \Delta P_{ext} + \Delta P_{DB} \tag{3}$$

A pressure balance was then established. The available pressure is dissipated by the energy loss, due to (i) the gas friction in the tube, although the related pressure drop is normally very low (<<1% of the total ΔP only) [8] and can be neglected; (ii) the energy loss due to the acceleration of the particles to conveying velocity; (iii) the energy loss, due to the friction of conveyed particles on the tube wall; and (iv) the energy loss, due to the weight of the particles in the column. These energy losses can be expressed in terms of their corresponding ΔP generated.

Combining all individual expressions with $\rho_s \alpha_p = G_s / U_s$, results in

$$\Delta P = \Delta P_{ext} + \Delta P_{\Delta B} = G_s U_s + g L \rho_s \alpha_p + \frac{3 C_D \rho_g L}{4 d_{sv} \rho_s} \frac{G_s}{U_s} \tag{4}$$

Since the particles in the tube are hindered by their surrounding dense particle phase, the terminal (free fall) velocity cannot be reached, and the effective "terminal" velocity will be a fraction of U_t only, as expressed in Eq (5).

$$\Delta U = U_g - U_s = K U_t \tag{5}$$

The proportionality constant K is a function of the bed voidage ($K = \varepsilon^n$), with exponent n cited in literature as 4.65 [9]. The experimental results favour the use of 4.65, which was hence accepted in Eq (6):

$$K = \varepsilon^{4.65} = (1 - \alpha_p)^{4.65} \tag{6}$$

The terminal velocity of particles in the laminar flow regime (certainly the case for group A powders) is given by:

$$U_t = [\frac{4gd_{sv}(\rho_s - \rho_g)}{3\rho_g C_D}]^{0.5} \tag{7}$$

The resulting equation relates G_s, U_g, U_t, k and ΔP:

$$Gs = \frac{\Delta P}{(U_g - KU_t) + \frac{K^2 gL}{(U_g - KU_t)}} \tag{8}$$

This transport equation reveals that for G_s to be positive, several conditions should be met:

(i) ΔP should exceed the sum of all operation-related energy losses.

(ii) U_g should exceed KU_t. Although $\alpha_p \leq 1$ and hence $K < 1$, this condition implies that operation of the upflow system cannot be secured at low values of the superficial air velocity.

(iii) The equation reveals that there will be a maximum in the (G_s-U_g) relationship. Setting $dG_s/dU_g = 0$ will determine the location of the maximum and results in $U_{max} \sim \sqrt{K^2 gL}$. For $K = 0.1$, $U_t = 0.2$ m/s and L= 1m, U_{max} = 0.33 m/s, which is beyond the terminal velocity implying that the conveying moves into a dilute pneumatic mode.

(iv) For potential UBFB applications, such as solar receivers, high operating gas velocities are prohibitive: the gas will leave the receiver at the discharge (top) particle temperature, hence contributing to sensible heat losses that need to be limited. At lower gas velocities, particle attrition and tube erosion will moreover be very limited.

Efficiency of the UBFB Conveyor System

The efficiency of the UBFB conveyor system can be calculated by comparing the compression and uplift work. To pressurize this air flow to the required pressure of the operating ΔP (in kPa) above the atmospheric pressure (101 kPa) work is needed in the compressor, W_s, according to Eq. (9), with η_c as compressor efficiency and k as ratio of specific heats of air $k = (C_p / C_y)$.

$$W_s = \frac{k}{k-1}(101)F_T[(\frac{101 + \Delta P}{101})^{\frac{k-1}{k}}]\frac{1}{\eta_c} \tag{9}$$

It should be remembered that the UBFB pressure drop itself is proportional the bed height, according to Eq. (2).

The work, W_r, required to lift the powder for a height L is

$$W_r = G_s \frac{\pi D^2}{4} L \frac{g}{10^3}, (in\ kW) \tag{10}$$

The efficiency of the upward conveying, η, is hence

$$\eta = \frac{Wr}{Ws} \times 100, in\ \% \tag{11}$$

The calculated efficiency is represented in Fig. 5.

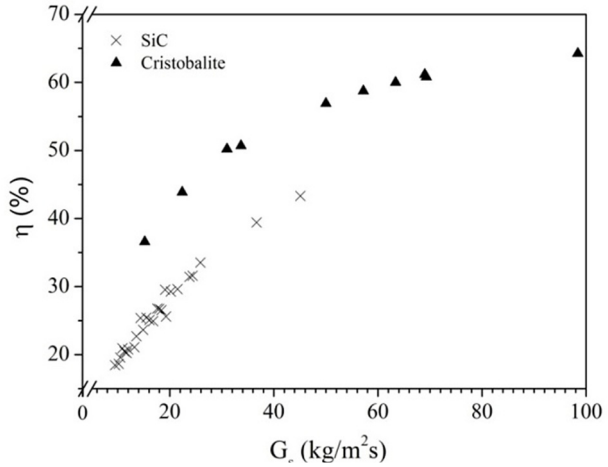

FIGURE 5: Calculated efficiency of the UBFB conveying.

A higher powder density (SiC versus cristobalite) reduces the conveying efficiency through the higher ΔP of the bed. For the same reason, a similar reduction of the efficiency will occur for deeper beds (longer tubes).

Slugging

Extensive research at ambient conditions demonstrated that wall slugging was found at a bed level of ~ 50 cm above the air inlet [10], whereas axi-symmetric slugging occurred at a height exceeding ~ 150 cm above the air inlet [11]. Slugs significantly reduce the bubble-induced particle mixing and associated excellent heat transfer. Photographic illustrations of the observed wall slugs are given in Fig. 6. A long UBFB will suffer from slugging both towards the wall-to-bed heat transfer coefficient, as towards the considerable pressure fluctuations measured across the bed.

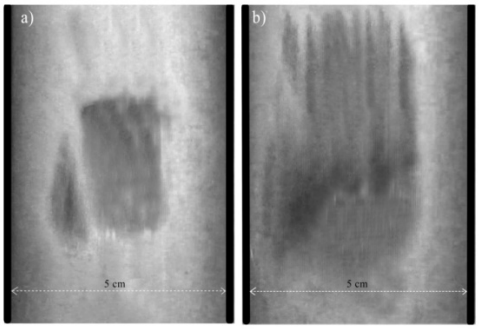

FIGURE 6: Wall slugs at the level of 90 cm in the bed: a) U-U_{mb} = 8.9 cm/s; b) U-U_{mb} = 11.4 cm/s

At higher temperatures, and in-line with predictions by Kong et al. [10], the onset of slugging is deferred to higher bed levels, as illustrated in Fig. 7. This finding is positive for the scaling up of the UBFB solar receivers that will involve multi-meter long tubes. Wall slugging is characterized by a slug frequency of 1 Hz. Axi-symmetric slugs move up the bed at a frequency of ~0.5 Hz.

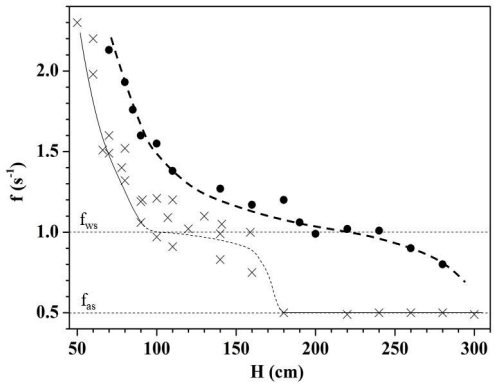

FIGURE 7: Bubble and/or slug frequency, f (s-1) versus level in the bed, x: ambient temperature, ●: at 475 °C.

The Maximum Achievable Solid Flux

Common fluidized bed operations can be hampered in a specific (U, G) range where choking occurs, being understood as the phenomenon where a small change in gas or solids flow rate prompts a significant change in the pressure drop and/or solids holdup: the stable upflow regime can no longer be maintained when G-values exceed a certain limit for a low to moderate gas velocity. This choking can occur in dense upflow of particles when the superficial gas velocity and the driving pressure are no longer capable of entraining the particles. In the upflow bubbling fluidized bed concept, only G-values up to 100 kg/m^{2}s were tested, where the stability of the operation was confirmed. This is expected since the pressure balance indicates that the loop will operate in a stable manner provided the external pressure in the dispenser compensates the upflow bubbling fluidized bed pressure drop. At high G-values, acceleration and friction losses, both proportional to G^n (n=1 to 2) [12] will increase and will finally hamper the system stability. To assess the impact of (U, G) combinations, a non-choking criterion is established when considering that the particle slip velocity must remain positive. With ε equal to 0.65 to 0.75, as measured in the single tube experiments, ρ_B is between 910 and 700 kg/m^3. For a specific gas velocity in the tube, the choking limit is illustrated in Fig. 8.

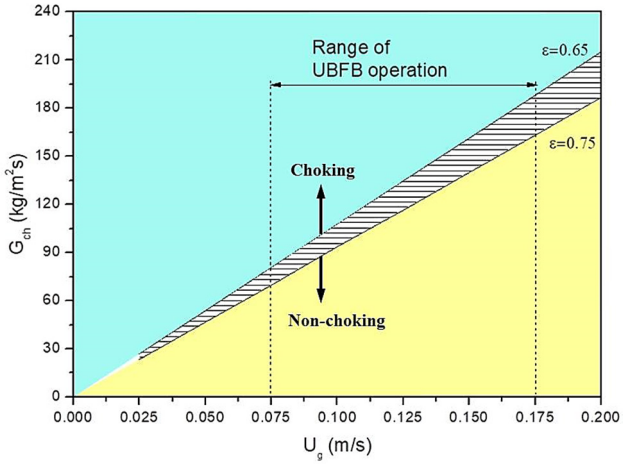

FIGURE 8: Predicted choking limit at different superficial gas velocities and bed voidages between 0.65 and 0.75

To operate the upflow bubbling fluidized bed at G-values in excess of 100 kg/m^{2}s, superficial air velocities should exceed 0.1 m/s, as commonly used in the single and multi-tube set-ups.

Attrition of Particles

Since a fluidized bed is the key in operating the solar receiver at a high wall-to-bed heat transfer coefficient, attrition of particles was examined experimentally in order to select the type of Geldart A-powders less prone to attrition. This extensive research was fully reported by Zhang et al. [13] and only essential features are summarized below. Although fast particle motion associates a high degree of mixing, it however causes inter-particle collision and bed-to-wall impacts, both leading to particle attrition. Attrition generates fines that can be lost in the dust collection system, whereas the particle size distribution of the bed will alter during the operation.

Zhang et al. clarified the influence of particle size and nature, bed height, fluidization velocity, action of jets and orifice diameter [13]. An equation was developed and enables to predict attrition rates for different particles at different operating contribution. The total attrition rate combines the bubble-induced and jet-induced effects. It was moreover shown that particles with a high Abrasion Index (AI), as defined by CEMA [14], are less prone to attrition. The higher AI is however an indication of the expected wear of the equipment [15]. Unlike SiC, cristobalite and olivine have a moderate AI and both attrition and erosion will be limited at the superficial gas velocities applied.

CONCLUSIONS

The UBFB is a key part of the novel solar power concept. The research has dealt with specific considerations in view of its scale-up, including: (i) the effect of the diameter of the receiver tubes and the use of internal fins; (ii) the applicable circulation flux; (iii) the possible extension of the pipe length from 0.5 or 1 m to beyond 3 m; (iv) the limited effect of powder attrition and equipment wear.

ACKNOWLEDGEMENTS

This work was supported by the Beijing Advanced Innovation Center for Soft Matter Science and Engineering of the Beijing University of Chemical Technology and funding was obtained from the European Union's Horizon 2020 research and innovation program under grant agreement 727762, project Next-CSP.

REFERENCES

1. G. Flamant, D. Gauthier, H. Benoit, J.-L. Sans, R. Garcia, B. Boissière, R. Ansart, and M. Hemati, Chem. Eng. Sci. **102**, 567 (2013).
2. B. Boissiere, R. Ansart, D. Gauthier, G. Flamant, and M. Hemati, Can. J. Chem. Eng. **93**, 317 (2015).
3. H.L. Zhang, H. Benoit, D. Gauthier, J. Degrève, J. Baeyens, I.P. López, M. Hemati, and G. Flamant, Appl. Energy **161**, 206 (2016).
4. I. Perez Lopez, H. Benoit, D. Gauthier, J.L. Sans, E. Guillot, G. Mazza, and G. Flamant, Sol. Energy **137**, 463 (2016).
5. H. Benoit, I.P. López, D. Gauthier, J.L. Sans, and G. Flamant, Sol. Energy **118**, 622 (2015).
6. H. Zhang, H. Benoit, I. Perez-Lopez, G. Flamant, T. Tan, and J. Baeyens, Renew. Energy **111**, 438 (2017).
7. H. Zhang, W. Kong, T. Tan, F. Gilles, and J. Baeyens, Sci. Rep. **7**, 10178 (2017).
8. K. Smolders and J. Baeyens, Powder Technol. **119**, 269 (2001).
9. K.M.S. Godard and J.F. Richardson, Inst. Chem. Eng. Symp. Ser. **30**, 126 (1968).
10. W.B. Kong, T.W. Tan, J. Baeyens, G. Flamant, and H.L. Zhang, Ind. Eng. Chem. Res. **56**, 4136 (2017).
11. F. Sabatier, R. Ansart, W. Kong, H. Zhang, J. Baeyens, and O. Simonin, Chem. Eng. Sci. Under final review (2018).
12. D. Kunii and O. Levenspiel, *Fluidization Engineering*, second edi (Butterworth-Heinemann, Newton-MA (USA), 1991).
13. H.L. Zhang, J. Degrève, J. Baeyens, and S.-Y. Wu, Powder Technol. **287**, 1 (2016).
14. M. Fayed and L. Otten, editors , in *Handb. Powder Sci. Technol.* (Springer, 2013), pp. 445–450.
15. C. Vandewalle and J. Baeyens, Powder Handl. Process. **13**, 77 (2001).